Indian Journal of Chemical Technology
Vol. 24, March 2017, pp. 206-212

Adsorptive desulfurization of model fuel by activated oil palm shell

S M Anisuzzaman*, Sariah Abang, Duduku Krishnaiah & MAR Razlan

Chemical Engineering Programme, Universiti Malaysia Sabah, 88400 Kota Kinabalu, Sabah, Malaysia

E-mail: anis_zaman@ums.edu.my

Received 20 December 2014; accepted 10 October 2016

The suitability and effectiveness of oil palm shells (OPS) as low cost adsorbents via physical activation for desulphurization of a model fuel under different concentrations have been studied. Batch mode experiments have been conducted to remove benzothiophine (BT) concentrations from the model fuel prepared from n-octane and p-xylene. The activated carbon (AC) has been characterized with fourier transform infrared spectroscopy (FTIR), scanning electron microscopy (SEM). The specific surface area and the pore-size distribution are determined using the Brunauer, Emmet and Teller (BET) and Barret, Joyner and Halenda (BJH) methods, respectively. The surface area is found to be 15.41 m2/g while total pore volume is 0.028cm3/g. The activated OPS is categorized as mesophorous adsorbent since the average pore size is 4.2 nm. The equilibrium data is best described by the Langmuir isotherm model and maximum adsorption capacity of this adsorbent is 2.75 mg/g. In addition, the rate of adsorption of BT is found to follow the pseudo-second-order kinetic model.

Keywords: Desulfurization, Oil palm shell, Adsorption, Sulphur-containing compound, Activated carbon

Apart from carbon and hydrogen, sulphur is the third most abundant element exists in the fossil fuel. It consists of four groups which are sulphides, mercaptans, disulphides and thiophenes[1]. The combustion of fuel oil, containing sulphur compounds emits sulphur dioxide (SO_x)causing air pollution and acid rain. Furthermore, it is also a poison in the catalytic convertors which is used to reduce carbon monoxide (CO) and nitrogen dioxide (NO_x) in the exhaust fume. In this case, the sulphur acts as an inhibitor where it competes with the exhaust pollutants, as it occupies the active sites of the catalyst.

Since sulphur is harmful to the environment, there are restrictions regarding the quality of fuels and the emissions from the refinery as well as the transportation fuel. The major goal of the regulations by the Environmental Protection Agency (EPA) is to reduce the sulphur content in transportation fuel. Currently, the sulphur level is 500 ppm in several countries. However, some countries have rigid pecifications. Ultra low sulphur diesel (ULSD) fuel of less than 50 ppm became the specification in both the European Union and Japan in 2005. The European Commission further adopted a 10ppm sulphur specification for road diesel fuel during 2005 with full conversion by 2010. On the other hand, sulphur oxides (SO_x) can react with other compounds in the atmosphere to form various harmful particles. These particles penetrate deeply into sensitive parts of the lungs and can cause or worsen the respiratory diseases, such as emphysema and bronchitis, and can aggravate existing heart disease, leading to increased premature death.

The technologies of sulphur removal have been developed in petroleum industries. In this field, the major process of removing sulphur is hydrodesulphurization (HDS). CoMo or NiMo catalyst was used in the recent HDS process at high temperature (320-380^oC) and high pressure (3-7 MPa)[2]. Alkyl dibenzothiophene (DBT) is the major compound existing in current commercial diesel with 4- or 6-position of alkyl group. HDS is very effective in removing thiols and sulfides, but it is not effective for the removal of thiophenic compounds. Among the unreacted refractory species are 4-methyl-dibenzothiophene (4-MDBT) and 4,6-dimethyldibenzothiophene (4, 6-DMDBT). The problem arises when the reduction of sulphur is dictated mainly by 4,6-dimethyldibenzophene where less reactive sulphur compounds substituting between both 4- and 6- alkyl groups[3]. Thus, the existing HDS technology to reduce the sulphur content to less than 10 ppm is not efficient and very costly.

In order to overcome this problem, there are some alternative technologies that have been developed. Processes such as oxidative desulphurization,

biodesulphurization and absorptive desulphurization are being considered for the purpose of removing sulphur content in diesel fuel[4]. Adsorption is one of the methods which can be used to achieve ultra-low sulphur content in diesel fuel. The adsorption is the most effective method in sulphur removal in fuels after HDS treatment[5].

Activated carbon (AC) is the common adsorbent used in the adsorption process[6]. This is due to their very high surface areas, large pore volumes, and tunable surface properties by introducing functional groups. The specific surface areas and porosities of AC are greatly affected by the precursors of carbonaceous materials and the preparation methods. In most cases, AC were used for the adsorption of compounds with weaker polarity from gas-phase or polar fluid phase such as the adsorption of organics in wastewater[7]. There are several materials that have been used in the fabrication of commercial AC as adsorbent for example lignite, coal, wood, and various agricultural and forest by-products with either using physical or chemical method[8-11]. Gases such as nitrogen (N_2) and carbon dioxide (CO_2) are used in physical activation while chemical activation with dehydrating agents such as zinc chloride ($ZnCL_2$), and potassium hydroxide (KOH) for the impregnation of the AC[12].

A low cost and promising adsorbent was recently studied especially on the agricultural waste such as oil palm shell (OPS)[13]. OPS is an abundantly available carbonaceous by-product from palm-oil processing mills in some tropical countries like Malaysia, Indonesia and Thailand. Preparation of adsorbents from the OPS is an economical and environmentally friendly utilization of these solid wastes. There are few studies that have made for the production of adsorbent from OPS[14-18].

Thus, this study is mainly focusing on the study of adsorptive desulphurization using AC derived from the OPS. The ability of the AC in desulphurization was studied with different adsorbent dosage, model fuel concentration and time. Consequently, the result was analyzed from the kinetics of the adsorbent to determine the performance of the AC.

Experimental Section

Preparation of model fuel

Stock solutions (10,000 mg/L each) for a model fuel were prepared separately for the adsorbate (99% benzothiophene (BT)) by dissolving them in a mixture of 75% v/v n-octane and 25% v/v p-xylene[19]. The solution with the fixed concentration of sulphur containing compounds (SCCs) which contained 10, 20, 30, 40 and 50 mg/L of BT were used. Combined solutions with same concentrations were prepared by successive dilution and mixing of the three solutions based on the following equation:

$$M_1V_1 = M_2 V_2 \quad \ldots(1)$$

where M_1 is the initial molarity, V_1 is the initial volume, M_2 the molarity and the V_2 volume.

Preparation of adsorbents

OPS was obtained from SawitKinabalu,

Kota Marudu, Sabah, Malaysia. The OPS was dried in an oven at 110°C for 24 h to reduce the moisture content. The dried samples were then grinded and sieved to a particle size fraction of 1.4-2 mm. Both carbonization and activation processes were carried out in a stainless steel tubular horizontal furnace. During carbonization, the starting material was placed on a metal crucible in the reactor under a nitrogen atmosphere. The furnace temperature maintained at 600°C, held for 3 h and then cooled to the room temperature (25°C). The resulting char was then activated at 600°C for 30 min with carbon dioxide (CO_2) at a rate of 100 cm^3/min to produce the activated OPS. Figure 1 presents the experimental set up for the production of activated OPS.

Adsorption experiment

For every adsorption experiment, 10 mL of solution with different model fuel concentration and adsorbent with same dosage (0.1 g) were placed in a beaker and magnetically stirred for a predetermined time (2-60 min). The adsorption temperature was maintained at 25°C and the stirrer was set to the speed of 5 rpm. After adsorption, the solution was separated from the solid with a syringe. The filtered solution was then analyzed with Agilent 6890B, USA gas chromatography

The amount of adsorption at equilibrium, (mg/g) was calculated as:

$$qe = \frac{(C_o - C_e)V}{W} \quad \ldots (2)$$

where C_o and C_e are the initial and equilibrium adsorbate concentration (mg/L), V is the volume of the solution (L) and W is the weight of activated carbon used (g).

Functional groups determination

Fourier Transform Infrared (FTIR) was used to analyze the functional groups present on the adsorbent of raw, carbonized and activated OPS. IR spectra was obtained with a type Spectrum 100 series FTIR spectrometer (Perkin-Elmer) using the transformation of 20 scans with a spectral resolution of 4 cm^{-1} by attenuated total reflectance method. FTIR spectra were collected in the mid infrared region between 4000 and 650 cm^{-1}. Spectra were acquired using air background correction.

Morphological characterization

Spectrometry electron microscopy **(**SEM)(Jeol JSM-5610LV, Japan) at 10 kV was used for the characterization of the morphology of the surface of the raw and activated OPS. Samples were mounted on self-adhesive carbon sticky tape and gold coated before imaging (JFC-1600 auto fine coater operated at 20 mA for 120 sec, Japan)

Specific surface area and pore-distribution

The specific surface area and the pore-size distribution were determined using the Brunauer, Emmet and Teller (BET) and Barret, Joyner and Halenda (BJH) methods, respectively. BET nitrogen isotherms were determined from the adsorption of nitrogen gas, N_2 at 150°C using a Quantachromeautosorbautomated gas sorption instrument, USA.

Results and Discussion

The FTIR spectra of raw OPS, char and AC samples was obtained based on the spectrum of raw OPS FTIR, the significant peak is observed at peak 2333 cm^{-1} which indicates the presence of O=C=O which is CO_2, and at peak 1021 cm^{-1} indicates the presence of Si-O-Si group which is silicon dioxide. On the other hand, the silica group is also present on carbonized OPS. For activated OPS, the band that is observed at 3702 cm^{-1} which indicates the presence of N-H (amine group) at 2345 cm^{-1} also indicates the presence of O=C=O which is CO_2. This is probably due to the incorporation of heteroatoms, oxygen atoms from enriched CO_2 atmosphere during the activation process within the carbon matrix. However, the surface functional groups of AC derived from OPS were generally neutral or slightly acidic[17].

Figure 2 shows the SEM micrographs of the raw OPS and the derived AC respectively. The surface of

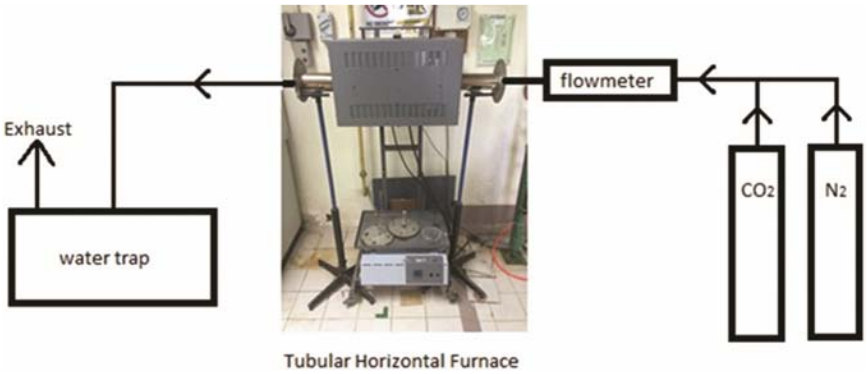

Fig. 1 — Experimental set up for the production of activated OPS

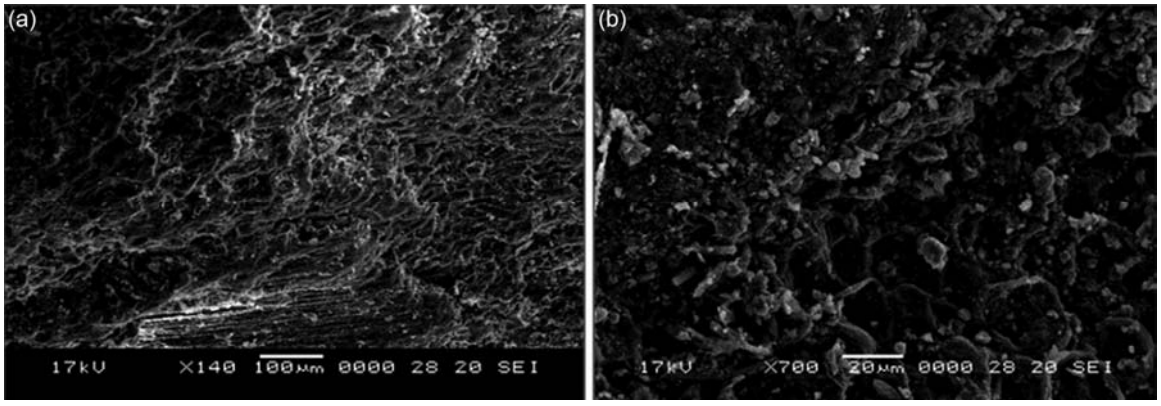

Fig. 2 — SEM micrograph of (a) raw OPS surface (b) activated OPS surface

the raw material is dense and planar without any cracks and crevices. This is one of the reasons for its poor or negligible BET surface area. The wood grain could be seen clearly on the surface since the OPS is a typical lignocellulosic structures materials. In contrast, the AC showed many small cavities forming a system of pore network. Thus, the AC has larger BET surface area and micropore surface area than the raw OPS[20].

The pore-size distributions of activated OPS indicate that large-diameter pore developed in the prepared AC. The pores of AC were divided into three types; small mesopores with diameters of 2-5 nm, large mesopore with diameters of 5-50 nm and large pores and channels with diameters over 50 nm, which form macropores[10,11,21].

The comparison between the pore-size distribution, BET specific area and total volume is shown in Table 1. It shows that the BET surface area is increasing from raw, carbonized and activated OPS in the range 0.69-15.41 m^2/g. Table 1 also shows that higher mesopore volume for activated OPS samples (0.028 cm^3/g) compare to raw OPS (0.0047 cm^3/g). Hence it can be concluded, activation by CO_2 enhances the surface area and micropore volume.

Effect of contact time

The effect of initial concentration, C_o on the adsorption capacity *qt* as a function of time was studied. Figure 3 shows the effect initial concentration of BT on the adsorption of capacity at 25°C. It is observed that for each initial concentration, the rate of adsorption is rapid for the first 25 min. After 35 min, the adsorption attained the equilibrium state where the rate of adsorption is almost constant. This is due to the fact that at initial stage, total surface area were available for adsorption and as the adsorption proceeds, more surface occupied thus the adsorption capacity decreased[6].

Based on the result, it can be observed that the interaction between the adsorbate and the activated OPS is enhanced by increasing the initial concentrations. Figure 3 also shows that the amount of BT adsorbed, *qt* is increased from 0.955-2.553 mg/g with an increase of BT concentration of 10-50 mg/L.

Effect of initial concentration on percent removal of benzothiophene

Table 2 shows the adsorption isotherm data of BT. Based on Table 2, it shows that the percentage removal of BT from the model fuel is decreased from 91.50-51.06% with an increase of initial concentration of BT from 10-50 mg/L. This may be due to the saturation of BT on the adsorption surface of the activated OPS as the concentrations were increased.

Adsorption isotherm study

The adsorption isotherm indicates how the adsorption molecules distribute between the liquid phase and solid phase when the adsorption process is reached an equilibrium state. The analysis of the isotherm is by fitting the data into different isotherm models, which is an important step for getting the suitable model that can be utilized for design purpose. Several equilibrium models have been developed to describe adsorption isotherm relationships. Two isotherm equations were tested in this study; these are Langmuir and Freundlich

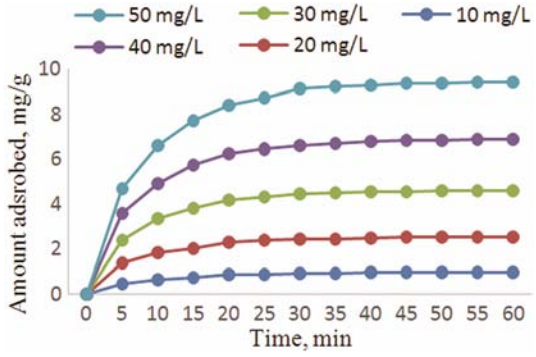

Fig. 3 — Amount of benzothiophene adsorbed as a function of time for activated OPS at 25°C

Table 1 — Summary of BET analysis

Sample	BET specific surface area, m^2/g	Average pore diameter, nm	Total volume, cm^3/g	Micropore volume, cm^3/g
Raw OPS	0.69	27.17	0.0047	0.0019
Carbonized OPS	11.39	7.04	0.0201	0.0054
Activated OPS	15.41	4.22	0.0280	0.0073

Table 2 — Adsorption isotherm data of BT

Initial concentrations, mg/L	Removal percentage, %	Equilibrium concentrations, mg/L	Amount adsorbed at equilibrium, mg/g
10	91.50	0.85	0.92
20	78.55	4.29	1.57
30	68.17	9.55	2.05
40	57.23	17.11	2.29
50	51.06	24.47	2.55

isotherm. The applicability of the isotherm models was assessed by the correlation coefficients, R^2 value of each plot.

Based on Table 2, it was also observed that adsorption capacity increases as the corresponding equilibrium concentration increases. This isotherm is used to determine the suitable type of adsorption isotherm for the activated OPS.

The Langmuir isotherm is shown in Fig. 4 (a). The equation 3 is the linear equation form Langmuir isotherm. It was used to determine the adsorption capacity, Q_{o} , Langmuir constant, K_L and separation factor, R_L using equation4, respectively:

$$\frac{C_e}{q_e} = \frac{1}{Q_o}\frac{1}{K_L} + \frac{1}{Q_o}(C_e) \quad \ldots (3)$$

$$R_L = \frac{1}{1 + K_L C_O} \quad \ldots (4)$$

Based on the Fig. 4 (a), the values of Q_O and K_L are 2.75 mg/g and 0.366 L/mg respectively. In addition, the value of is 0.9942 while the separation factor, value is 0.498 which is in the range of 0 to 1, thus it is favourable.

The linear equation of Freundlich isotherm is used to determine the adsorption capacity indicators, (L/g) and adsorption intensity, n by the following relation:

$$\log q_e = \frac{1}{n}\log C_e + \log K_F \quad \ldots (5)$$

The experimental results of and are shown in Fig. 4 (b). It shows the slope value, which is 0.3055 and that gives the value of n, which is 3.273. Generally, n> 1 suggests that adsorbate is favorably adsorbed on the adsorbent. The y-intercept from the graph is -0.0074. The value of K_F is 0.983 L/g while the R^2value is 0.9924.

As a comparison, the correlation value of for Langmuir isotherm is slightly higher than the Freundlich isotherm. It shows that the activated OPS fit the Langmuir model which is favourable for monolayer adsorption. As shown by Langmuir isotherm, the adsorption capacity is 2.75 mg/g which occupies almost 100% of total pore volume of 0.0280 cm^3/g of the adsorbent.

Kinetics study of adsorption

The mechanism and the efficiency of the adsorption process can be derived from their kinetic studies. Therefore, the kinetic data was processed in order to understand the kinetics of adsorption process in terms of order of the rate constant. The experimental data for the benzothiophene at different time intervals were examined in terms of pseudo-first-order and pseudo-second-order kinetics.

The pseudo-first-order kinetic model is widely used to predict the adsorption kinetics and is expressed as:

$$\log(q_e - q_t) = \log q_e - \frac{k_1}{2.303}t \quad \ldots(6)$$

where q_e and q_t (mg/g) are the amounts of adsorbate adsorbed at equilibrium and at time interval, t (min), respectively. t (min^{-1}) is the adsorption rate constant. In order to determine the suitability of the experiment data with pseudo-first-order kinetic model, a graph of log (q_e-q_t) versus t was plotted as shown in Fig. 5 (a).

On the other hand, the pseudo-second-order equation predicts the behavior over the whole range adsorption and is expressed as:

$$\frac{t}{q_t} = \frac{1}{k_2 q_e^2} + \frac{1}{q_e}t \quad \ldots (7)$$

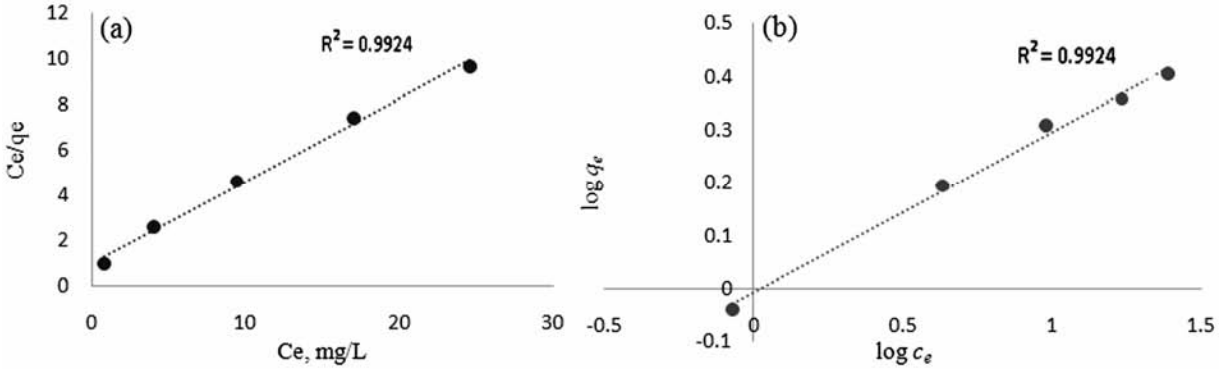

Fig. 4 — (a) Langmuir isotherm (b) Freundlich Isotherm

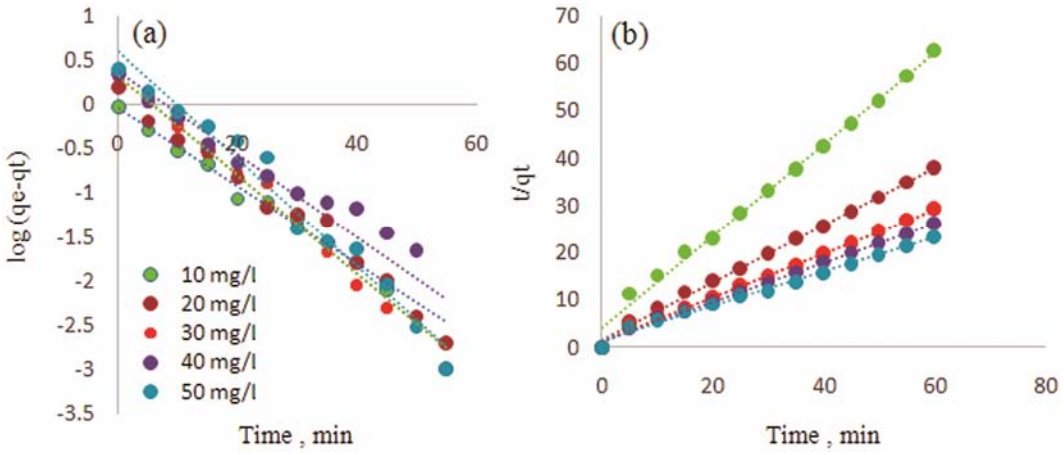

Fig. 5 — (a) pseudo first-order plot (b) pseudo second-order plot

Table 3 — Kinetics study of activated OPS

Initial concentration, mg/L	q_e, exp, mg/g	Pseudo-first order			Pseudo-second order		
		q_e, cal , mg/g	k_1	R^2	q_e, cal, mg/g	k_2	R_2
10	0.955	0.891	-0.101	0.9905	1.068	0.157	0.9982
20	1.571	1.460	-0.114	0.9852	1.649	0.214	0.9970
30	2.045	2.032	-0.128	0.9933	2.164	0.152	0.9958
40	2.289	2.292	-0.111	0.8884	2.412	0.123	0.9958
50	2.553	3.866	-0.139	0.9730	2.770	0.081	0.9917

where k_2 (g/mg.h) is the rate constant of second-order adsorption. Table 3 summarized and compared both kinetic models. In order to determine the suitability of the experiment data with pseudo-second-order kinetic model, a graph of versus t was plotted (Fig. 5 (b)).

By comparing the two graphical charts in Fig. 5 (a,b), it was observed that the correlation coefficients (R^2) for pseudo-second-order model are closer to unity, and hence indicating a better fit with the pseudo-second-order model. The correlation coefficients (R^2) for pseudo-second-order are in the range of 0.9917 to 0.9982, which are higher than the the pseudo-first-order (0.8884 to 0.9933). Hence, the adsorption process of BT using activated OPS adsorbent is said to follow pseudo-second-order kinetic model. Moreover, this also suggests that chemisorptions might be the rate-limiting step that controls the overall adsorption process[16,22].

Conclusion

The results of the experiments and investigations, together with the findings of the analysis, have shown that AC derived from OPS is a promising adsorbent to be used in the removal of BT over at low range of concentrations. OPS can be used as an alternative adsorbent to replace conventional AC in removing low concentration BT. Besides, relatively low cost also makes it a promising non-conventional adsorbent to be used in the industry. From the experiments carried out, adsorption of BT has found to be increased with increase in initial concentration of BT. The adsorption capacity of the adsorbent increased steadily with the increase in initial BT concentration. On the other hand, the percentage removal of BT from the model fuel is decreased from 91.50% to 51.06% with an increase of initial concentration of BT from 10 mg/L to 50 mg/L. The equilibrium data is best described by the Langmuir isotherm model. Maximum adsorption capacity of this adsorbent is 2.75 mg/g. In addition, the rate of adsorption of BT is found to follow the pseudo-second-order kinetic model with promising correlation of $0.9917 < R < 0.9982$. In overall, activated oil palm shell is capable in removing low concentration of sulphur-containing compound such BT from model fuel.

Acknowledgement

The authors wish to acknowledge the financial support from University Malaysia Sabah (UMS) under the UMS grant number SBK0150-TK-2014.

References

1 Adeyi A A & Aberuagba F, *Res. J Chem Sci*, 2 (2012) 14.
2 Kim J H, Ma X, Zhou A & Song C, *Catal Today*, 111 (2006) 74.
3 Song C, *Catal Today*, 86 (2003) 211.
4 Dasgupta S, Gupta P, Aarti A, Nanoti A N, Goswami M O, Garg E, Tangstad B, Vistad A, Karlsson M & Stocker, *Fuel*, 108 (2013) 184.
5 Muzic M, Sertic-Bionda K, Gomzi Z, Podolski S & Telen S, *Chem Eng Res Des*, 88 (2010) 487.
6 Krishnaiah D, Anisuzzaman S M, Bono A & Sarbatly R, *J King Saud Univ Sci*, 25 (2013) 251.
7 Bu J, Loh G, Gwie C G, Dewiyanti S, Tasrif M & Borgna A, *Chem Eng J*,166 (2011) 207.
8 Hayashi J, Horikawa T, Takeda I, Muroyama K & Ani F N, *Carbon*, 40 (2002) 2381.
9 Mui E L K, Ko D C K & McKay G G, *Carbon*, 42 (2004) 2789.
10 Anisuzzaman, S M, Joseph, C G, Taufiq Yap, Y H, Krishnaiah D & Tay V V, *J King Saud Univ Sci*, 27 (2015) 318.
11 Anisuzzaman, S M, Joseph C G, Daud W M A W, Krishnaiah D & Yee H S, *Int J IndChem*, 6 (2015), 9.
12 Sumathi S, Bhatia S, Lee K T & Mohamed A R, *Bioresour Technol*, 100 (2009) 1614.
13 Anisuzzaman S M, Krishnaiah D, Abang S & Labadin G M, *J Appl Sci*, 14 (2014) 3156.
14 Adinata D, Daud W M A W, Aroua M K, *Fuel Process Technol*, 88 (2007) 599.
15 Daud W M A W & Ali W S W, *Bioresour Technol*, 93 (2004) 63.
16 Foo K Y & Hameed B H, *Bioresour Technol*, 111 (2012) 425.
17 Guo J & Lua A C, *Chem Eng Res De*, 81 (2003) 585.
18 Lua A C & Guo J, *J Environ Eng*, 127 (2001) 895.
19 Ahmed I, Khan N A, Hasan Z & Jhung S H, *J Hazard Mater*, 250-251 (2013), 37
20 Guo J & Lua A C, *Mater Lett*, 55 (2002) 334.
21 Wang J, Yang X, Wu D, Fu R, Dresselhaus M S & Dresselhaus G, *J Power Sources*, 185 (2008) 589.
22 Cazetta A L, Vargas A M M, Nogami E M, Kunita M H, Guilherme M R, Martins A C, Silva T L, Moraes J C G & Almeida D C, *Chem Eng J*, 174 (2011)117.